

## MEASUREMENTS ON PULSED SUPERCONDUCTING DIPOLE MAGNETS

J H Coupland and D E Baynham  
Rutherford Laboratory  
Chilton, Didcot, Berkshire, England

### Abstract

Measurements of the magnetic field in the bore of two superconducting dipole magnets are discussed after a brief description of the magnets, AC3 and AC4. The achieved field uniformity in the useful aperture of the iron yoked magnet AC4, though not yet sufficient, is approaching that required for a proton synchrotron. In the absence of any compensation of the remanent field, the rather large sextupole component, rising to 0.6mT at the edge of the useful aperture in AC3 and 1.2mT in AC4, will impose a lower limit on the injection energy into the synchrotron ring.

### 1. Introduction

This report is primarily about the field measurements that have been made to date on superconducting dipole magnets, but before describing these it is helpful by way of introduction to mention the general context of this work. The magnets AC3, AC4 and its successor AC5 are part of the current programme<sup>1</sup> at the Rutherford Laboratory to demonstrate the feasibility of pulsed superconducting magnets as elements in an extra high energy proton synchrotron, either in the conversion of an existing accelerator or in the building of a completely new one. As the magnets AC3 and AC4 differ in many respects a brief description of the design and construction is given first in each case.

The field measurements and their analysis depend on the stepwise movement of a detector, which is either a search coil coupled to an electronic integrator or, additionally at low fields, a peaking strip, which is particularly useful in distinguishing between the remanent field due to super-currents, and remanent magnetisation in the construction-materials of the coil, cryostat and environment. Long search coils are used to obtain half integrals of the transverse field taken along paths parallel to the magnet axis.

In the Appendix formulae are derived for the theoretical estimation of the remanent field for a magnet with sector windings surrounded by a circular iron shield.

### 2. The Magnet AC3

#### 2.1 General Description

This magnet, is an example of the style of design advocated<sup>2</sup> at the last magnet conference. At that time studies in the Rutherford Laboratory were aimed at the possibility of converting the 7 GeV proton synchrotron NIMROD into a 25 GeV accelerator by replacing the existing magnets with superconducting ones. To achieve this goal would

have required dipoles of at least 6 T field in a new separated function lattice arrangement. To obtain the maximum energy the effective length of the dipole magnets, or  $\int B_y dl$ , has to be as large as possible along the fixed beam path length available, a requirement which favours 'bedstead ends'. This type of end is easy to wind, it does not raise a peak field, and when used in conjunction with sector geometry automatically leads to a good quality field integral. It was also considered desirable to have an external iron shield, but in view of the high central field of the magnet locate it at a distance, most conveniently to enclose the end windings in this case. However, it is now suggested by more recent calculations<sup>3</sup> that the iron can be placed close to the coils and still obtain a good field quality over the range 0 to 6 T, cf. also the arrangement in AC4.

Since the magnets have to be pulsed, there is a volumetric heat source in the windings and deliberate low resistance heat paths have to be arranged to conduct this heat to the coolant liquid helium. AC3 employs conducting mats made from electrically insulated copper wires, often called 'heat drains', which are placed between the layers so as to transport heat azimuthally in the side sections and radially in the end windings, see Fig. 1 for a sectional drawing of the windings. In operation the magnet is mounted vertically in a tub cryostat.

#### 2.2 Performance

The magnet was completed last year by a team led by M N Wilson who has already reported on its successful testing under pulsed conditions. The ac loss, about 50J/cycle, was roughly as expected and increased significantly for rise times shorter than one second. More details of the magnet and these tests were given in the paper by M N Wilson et al<sup>4</sup>. The magnet has also been run with two additional inner pancake coils which raised the maximum central field from 3.9 to 4.5 T. No external iron shield was used. Very low field measurements using peaking strips showed that the coil assembly changes shape on cool down and further evidence that the coil moved under excitation was provided by the distorted shape of the coil hysteresis loop, a plot of  $\int V dt$  against current, where V is the 'backed off' coil voltage. The whole assembly was therefore clamped up very tightly before making the following field measurements.

The bore of the magnet is 10 cm dia., the overall length 40 cm, the inductance 4.8mH and with a current of 4,930 A gives 3.9 Tesla dipole field.

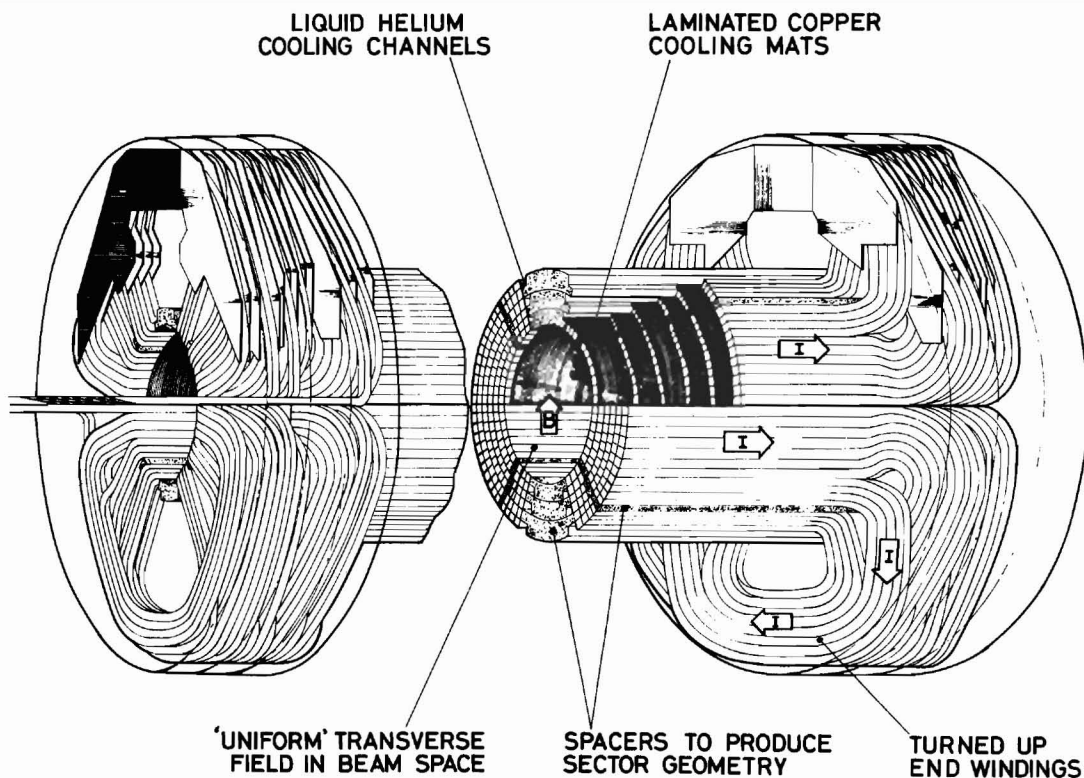


Fig. 1. Sectional drawing of the windings, AC3

### 2.3 Field measurements

Most of the measurements are made using two search coils mounted on a radial arm and moved in  $10^\circ$  azimuthal steps about the axis of the magnet. A difference signal is taken between one coil mounted at the centre and another at a large radius so as to enhance the sensitivity to the harmonics relative to the fundamental. The coil voltages are fed to an integrator and the flux changes Fourier analysed to obtain the normalised coefficients in the expression for  $B_r$ , the apparent radial field of the magnet,

$$B_r = B_0 \left[ P \sin(\theta - \phi_1) + C_2 \left( \frac{r}{a} \right) \sin 2(\theta - \phi_2) + C_3 \left( \frac{r}{a} \right)^2 \sin 3(\theta - \phi_3) + \dots \right],$$

where the fundamental is attenuated according to the relative turns area of the two coils, i.e.  $P = 1 - [NA]_b / [NA]_r$ ,  $r$  is the radius to the centre of the search coil and  $2a$  the aperture of the winding.

Except for the search coils and their leads, all the rest of the integrator, i.e. within the dotted region of Fig. 2, is placed in a dry constant temperature enclosure at  $30 \pm 0.1^\circ\text{C}$  to reduce drift. The integrator is based on a good

quality I.C. amplifier (Advance 148c) used in the operational mode with a low leakage  $1 \mu\text{F}$  condenser (Suflex SK602) to give a time constant  $RC$  of  $0.1 \text{ sec}$ . A zero drift correction is applied to the input and with low leakage components there was no further need for proportional control. Typical drift observed over a 10 min. interval is  $60 \mu\text{V}$ , or  $0.6 \mu\text{T/min}$  using coils of  $NA = 10^4 \text{ cm}^2$ . The measurements with AC3 show a consistency in harmonic coefficient of  $1$  in  $10^4$  confirming that the drift is acceptably small for present purposes.

Table 1 shows the harmonic coefficients  $C_n$  for five different field levels, 1, 2.0, 2.5, 3.0 and 3.4 T, where it is seen that there is little change in relative harmonic content with excitation. The magnet was wound with a large conductor, 5 mm square, and represents only a rather rough approximation to idealised 2 sector geometry. The calculated harmonics from the constructional drawings, shown in the last column, are only in fair agreement, but the rather large quadrupole and octupole terms, indicating a lack of symmetry, are greater than expected from known differences in coil construction.

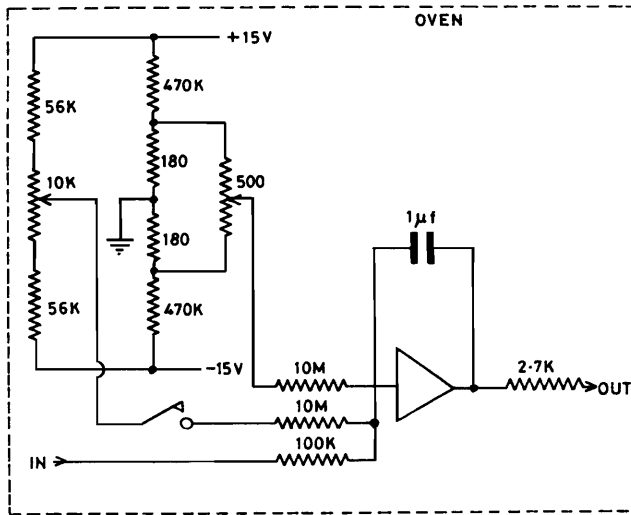


Fig. 2. Integrator

TABLE 1. AC3 Harmonic Coefficients  $C_n$  for Different Field Levels

(field in aperture,  $B_r = B_0 \sum C_n \left(\frac{r}{a}\right)^{n-1} \sin n(\theta - \theta_n)$ )

n	$B_0=1T$	$B_0=2T$	$B_0=2.5T$	$B_0=3T$	$B_0=3.4T$	Pre-dicted Values
1	1.0000	1.0000	1.0000	1.0000	1.0000	1.0000
2	0.0020	0.0022	0.0021	0.0021	0.0021	zero
3	-0.0178	-0.0178	-0.0178	-0.0176	-0.0176	-0.0235
4	0.0014	0.0015	0.0015	0.0015	0.0015	zero
5	-0.0090	-0.0090	-0.0090	-0.0091	-0.0090	-0.0131
6	0.0008	0.0007	0.0007	0.0006	0.0006	zero
7	0.0079	0.0077	0.0077	0.0082	0.0085	0.0117
8	0.0009	0.0009	0.0009	0.0012	0.0012	zero
9	-0.0247	-0.0248	-0.0249	-0.0251	-0.0248	-0.0330
10	0.0011	0.0008	0.0012	0.0009	0.0007	zero

## 2.4 Remanent Fields

Remanent effects in the useful aperture caused by trapped fields, or the magnetisation associated with persistent currents circulating up and down the filaments of the conductor, have been measured after AC3 has been excited to different levels and then brought back to zero and the circuit broken. That these fields might be important and impose a lower limit on the injection energy has recently been stressed by M Green<sup>5</sup> of Berkeley, who observed and analysed large remanent fields in a dipole magnet wound with Nb/Ti conductor having very large, 69 micron, filaments. The measurements for AC3 were made either with the search

TABLE 2  
AC3. Remanent fields after excitation to different values of central field,  $B_0$ .

Harmonic number, n	Remanent amplitudes at full aperture (mT)				Computed Values
	$B_0=0.5T$	$B_0=1T$	$B_0=1.5T$	$B_0=3.4T$	
1	0.454	0.479	0.491	0.514	0.297
3	1.028	1.056	1.046	0.953	0.607
5	-0.193	-0.184	-0.178	-0.207	-0.156
7	0.278	0.279	0.228	0.236	0.250
9	0.076	0.076	0.072	0.095	0.056

All even harmonics are less than 0.1 mT. The background has been subtracted in all cases.

coils just described for measuring the main field, or with peaking strips which have proved very convenient<sup>6</sup> for measuring low fields < 1.5mT, particularly since their calibration is independent of temperature. The second harmonic in the difference signal between the strip on the radial arm in the magnet and a similar cold fixed one outside the magnet gives the magnitude of the field. The results shown in Table 2 show little variation of harmonic content after magnet excitations to 0.5 T and above. Since it requires only 50 mT to fully penetrate the 8 micron filaments it is reasonable to assume in a theoretical analysis, as in the Appendix, that a magnetic moment M/unit volume is created throughout the winding, constant in magnitude but with a direction given by the local magnetising field. Although AC3 does not have an iron shield more general formulae applicable to a sector coil magnet with an iron shield are derived in the Appendix. The resulting double integral which has to be evaluated over the coil, can be simplified if it is assumed that the mean direction of the field in the winding, and hence M, at any azimuth is radial, which is a reasonable assumption for a thin air-cored coil. The harmonic ratios  $C_1/C_3$  and  $C_5/C_3$  so obtained agree fairly well with the experimental ratios and also those obtained from numerical evaluation of the double integral on the computer, though these latter values appear to be too small in absolute magnitude, if  $j_c$  is taken as  $10^{10} \text{ A m}^{-2}$ . These remanent fields are found to be unchanged over a period of half an hour.

## 3. The Magnet AC4

### 3.1 General Description

Freed from the limitations and objectives for AC3, this magnet by contrast embodies several of the design alternatives. It is conceived as a preprototype test design for a dipole magnet, 4.5T maximum field, to be used either in a conversion of one of the new multi-hundred GeV proton synchrotrons or in the con-

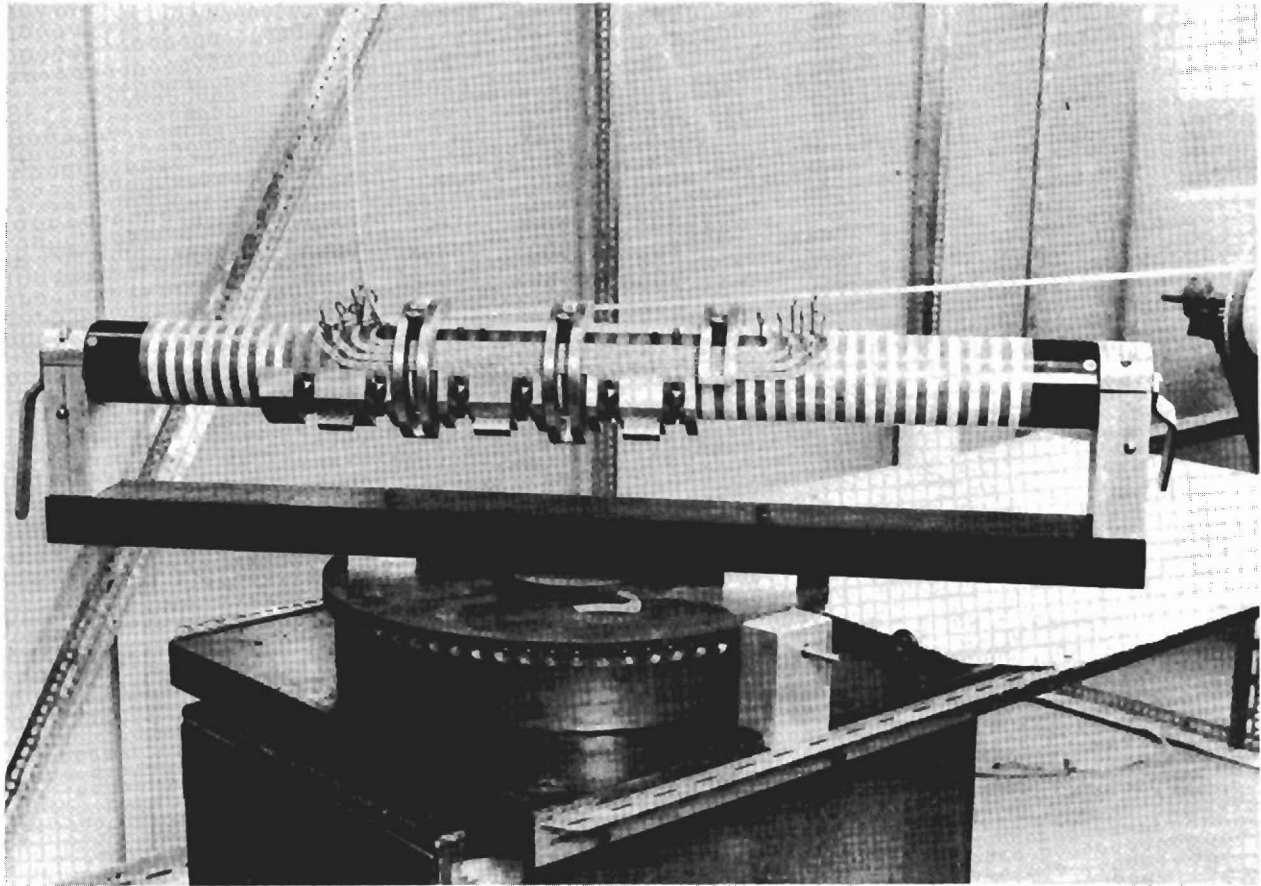


Fig. 3. Coil Winding

struction of a new 1,000 GeV ring. To obtain the most economical design the iron is closely associated with the windings as in Brookhaven designs<sup>7</sup> but shaped to control the effects of saturation. With this arrangement the iron contributes about a third of the total field. The design is of layer type<sup>8</sup> wound as two pairs of double pancakes, and like AC3 is based on circular mandrels so that the moulded coils nest together on assembly as a concentric unit, so simplifying relative alignment problems. The layers have smooth ends which are well spaced to limit the peak field rise, and in principle should give a good quality field integral as calculated by simple application of the integral Theorem<sup>9</sup>. In practice ideal angles have to be varied to obtain axial alignment of the helium channels layer to layer and hence provide common inlets and outlets. Despite these variations and others, for example non sharp bends in the conductors, a tolerably good end is achieved as evidenced by field integral measurements, see next section. The overall length of the coils is 0.72m. having 0.40m. straight sections.

Figure 3 shows coil winding in progress, and

Fig. 4 illustrates the assembly of the potted coils and iron yoke in prefabricated units. The iron yoke, assembled from stampings bonded together with epoxy resin, is split in the vertical direction for ease of assembly and clamping, having regard to differential thermal shrinkage on cool down: it also facilitates any dismantling at a later date as AC4 is intended as a sort of testbed.

For testing, the horizontal magnet is totally immersed in liquid helium in a large (1.22 m dia.) laboratory cryostat. The heat removal mechanism is by nucleate boiling in thin (10 mm x 0.8 mm) annular channels moulded into the windings between the layers and distributed throughout the length including the end regions as previously mentioned. The flow path for liquid and gas is up past the split faces of the iron laminations to enter the windings, then circumferentially through the lower pancakes and on through the upper ones to leave past the upper split faces of the iron. It is intended to describe this magnet in detail elsewhere at a later date when the magnet has been fully tested.

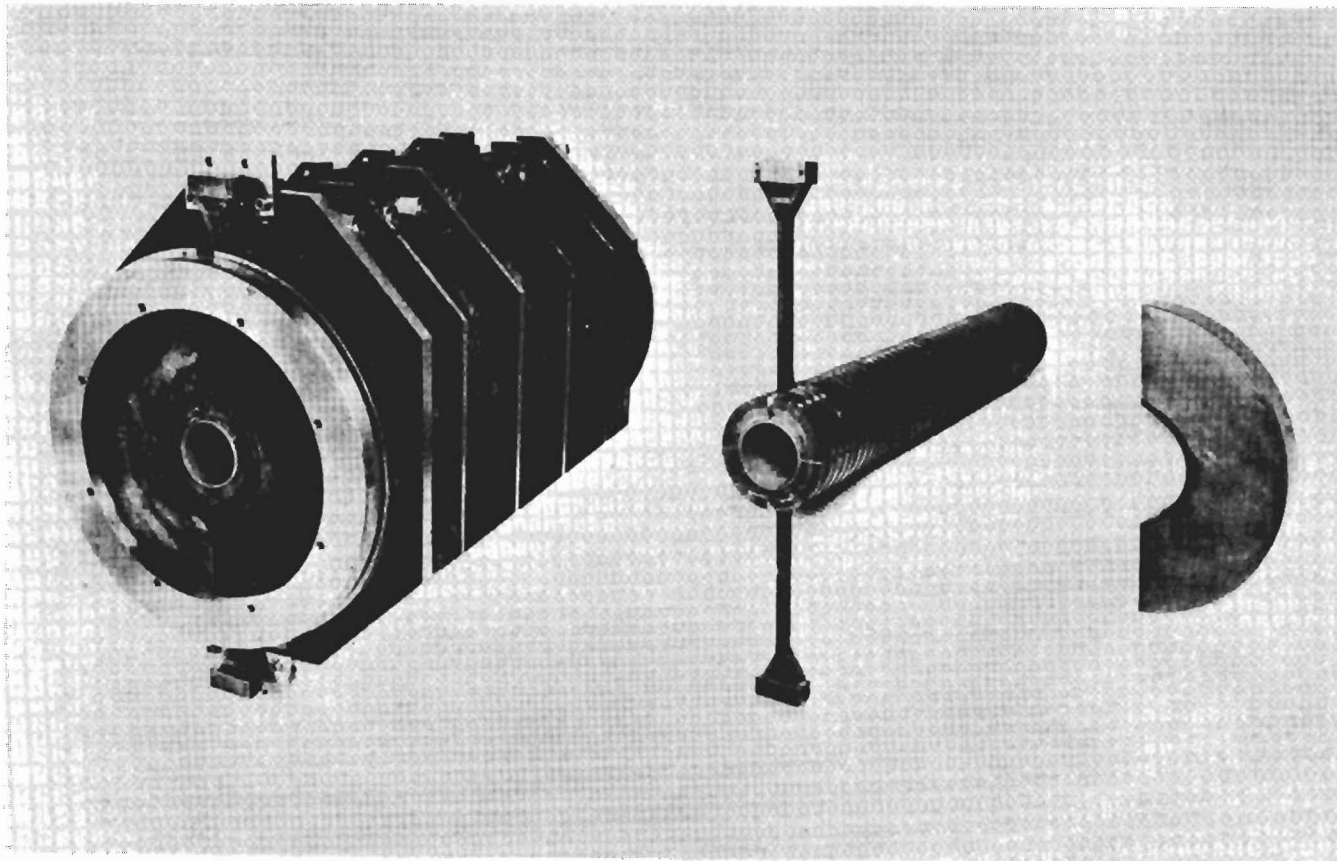


Fig. 4. Assembly of coils and iron yoke

### 3.2 Performance

The measurements reported are the first ones and are limited by the time available before this conference. The magnet reached the design goal of  $B_0 = 4.5$  T at 5.2 kA after training from 4.1 T. It also pulses to this current on a 4 second cycle, or 2 second rise time, and to 240 A less due to the increased heating when the cycle time is halved. The a.c. loss, by the method used for AC3, gives a total of 71 j/cycle (wt. of conductor = 16.4 kg, wt. of iron = 950 kg) for the 2 second cycle 0 to 4 kA to 0. Above this current the method becomes increasingly difficult as the sensitive voltage balance is upset by the iron going into saturation which is seen as a large spike on the usual "Isle of Wight" type hysteresis curve, see Fig. 5.

After excitation to the full field there is a total remanent field of, dipole = 1.2 (0.2), sextupole = 1.9 (0.0) and decapole = 0.4 (0.0) mT, where the figures in brackets relate to the non-superconducting part, ie. the iron yoke in this case. The filament diameter is 12 micron in the AC4 conductor.

### 3.3 Field Measurements

The same method, search coil and integrator, is used to measure the field at the centre and using long coils half integral measurements are made and analysed in a similar way into circular harmonics. However, to avoid stray fields in the laboratory and also to gain increased sensitivity, all measurements at very low currents are done with 50 Hz excitation with the integrator replaced by a rectifier circuit to measure the ac voltage picked up in the search coils.

Table 3 column II shows the field coefficients for very low excitation at room temperature without iron. Column III shows the coefficients also at room temperature but with the iron yoke in position. The half integral values are shown in brackets.

The difference in  $C_3$  is roughly as calculated though the comparison is a little indefinite as the coil is distorted in the clamped up condition at room temperature. However, the quadrupole is noticeably increased, suggesting that the assembled iron fits asymmetrically.

Column V is again at low excitation but cold, 77°K.

TABLE 3. AC4, Harmonic Coefficients,  $C_n$

n	Bare coils at 293°K	Coils with iron at 293°K	Coils with iron, 77°K
1	1.0000	1.0000	( 1.0000)
2	0.0011	0.0033	( 0.0028)
3	-0.0330	-0.0046	(-0.0052)
4	0.0020	0.0011	( 0.0010)
5	-0.0028	-0.0051	(-0.0063)
6	0.0002	0.0002	( 0.0008)
7	-0.0095	-0.0052	(-0.0009)
8	0.0031	0.0022	( 0.0009)
9	-0.0117	-0.0096	(-0.0014)
10	0.0030	0.0021	( 0.0005)

**MAGNETISATION CURVES AT 4 SECOND CYCLE TIMES**

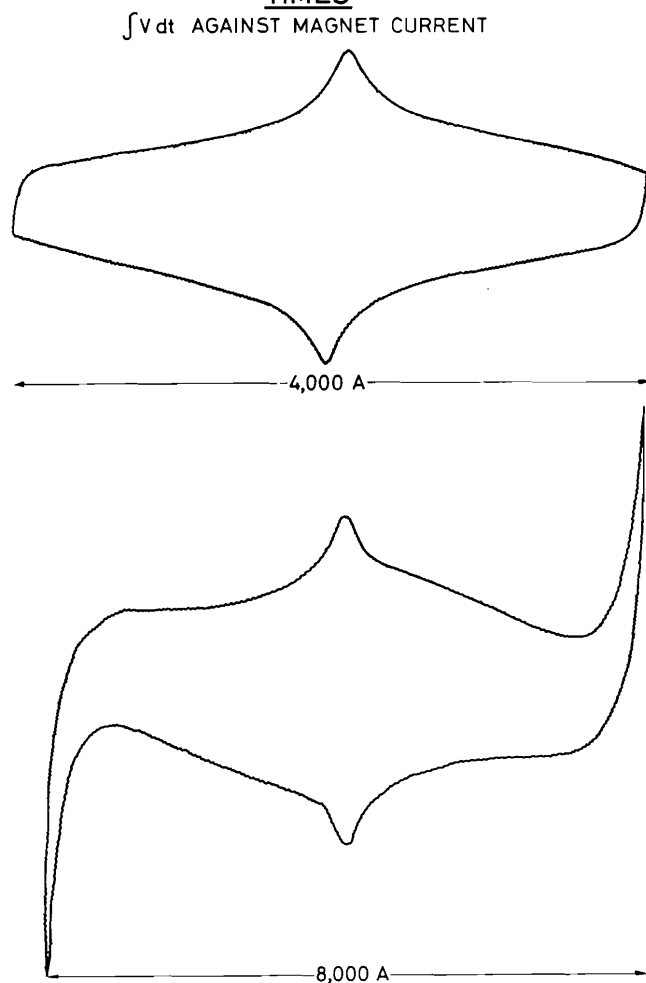


Fig. 5. Magnetisation curves

Table 4(a) shows the coefficients at different field levels, showing the effect of iron saturation. The expected values are given in Table 4(b).

These results confirm that the variation of harmonic coefficients with iron saturation is much as expected from computations<sup>3</sup> if a small outward movement of the coils occurs at the higher excitations but that the basic shape of the coil as manufactured and clamped in the assembly is incorrect.

Acknowledgements

We are grateful to R S Stovold and P T Clew and their colleagues for engineering work in the construction and commissioning of AC3 and AC4, and to N H Cunliffe, J Brown, V W Edwards, M Dean and R Kimber for their help in connection with the measurements.

References

1. P F Smith, Proc. 8th Int. Conf. on High Energy Accelerators, CERN 1971, p 44.
2. J H Coupland, Proc. 3rd Int. Conf. on Magnet Technology, Hamburg, 1970, p 157, or Rutherford Laboratory Print RPP/A88.
3. J H Coupland, J Simkin and T C Randle, Rutherford Laboratory Preprint RPP/A90(1972)
4. M N Wilson et al., Applied Superconductivity Conf. Annapolis 1972 (in the press).
5. M A Green, IEEE Trans. Nucl. Sci. NS-18, No. 3, 664 (1971).
6. D E Baynham, Rutherford Laboratory report (in preparation).
7. W B Sampson et al. Particle Accelerators, 1, 173, (1970).
8. A Asner and C Iselin, Proc. 2nd Int. Conf. on Magnet Technology, Oxford 1967, H Hadley, Editor (Rutherford Laboratory 1967) p 32.
9. J H Coupland, "Equations & Formulae for Magnets with Air Cored Windings of Saddle Coil Type", Rutherford Laboratory Report RHEL/R203 (H.M.S.O. 1970) p.15.

TABLE 4(a) AC4 Harmonic Coefficients  $C_n$  at Different Field Levels, Measured Values

Harmonic number, n	$C_n$ $B_o = 0.8T$	$C_n$ $B_o = 1.7T$	$C_n$ $B_o = 1.7T$	$C_n$ $B_o = 2.5T$	$C_n$ $B_o = 3.0T$	$C_n$ $B_o = 3.5T$	$C_n$ $B_o = 4.0T$	$C_n$ $B_o = 4.0T$
1	1.0000	1.0000	( 1.0000)	1.0000	1.0000	1.0000	1.0000	( 1.0000)
2	0.0035	0.0036	( 0.0033)	0.0036	0.0036	0.0035	0.0034	( 0.0030)
3	- 0.0050	- 0.0049	(-0.0046)	- 0.0048	- 0.0047	- 0.0045	- 0.0042	(-0.0042)
4	0.0009	0.0008	( 0.0007)	0.0008	0.0008	0.0008	0.0008	( 0.0007)
5	- 0.0050	- 0.0047	(-0.0056)	- 0.0046	- 0.0043	- 0.0039	- 0.0032	(-0.0048)
6	0.0009	0.0009	( 0.0006)	0.0008	0.0010	0.0009	0.0008	( 0.0005)
7	- 0.0040	- 0.0037	(-0.0014)	- 0.0038	- 0.0038	- 0.0040	- 0.0043	(-0.0015)
8	0.0005	0.0005	( 0.0003)	0.0005	0.0005	0.0007	0.0007	( 0.0003)
9	- 0.0027	- 0.0023	(-0.0008)	- 0.0023	- 0.0023	- 0.0023	- 0.0023	(-0.0010)
10	0.0018	0.0012	( 0.0003)	0.0006	0.0012	0.0018	0.0018	( 0.0016)

TABLE 4(b) AC4 Expected Values

Harmonic number, n	$C_n$ $B_o = 0.8T$	$C_n$ $B_o = 1.7T$	$C_n$ $B_o = 2.5T$	$C_n$ $B_o = 3.0T$	$C_n$ $B_o = 3.5T$	$C_n$ $B_o = 4.0T$	$C_n$ $B_o = 4.5T$
1	1.0000	1.0000	1.0000	1.0000	1.0000	1.0000	1.0000
2	zero	-	-	-	-	-	-
3	0.0000	0.0000	0.0000	0.0001	0.0006	0.0011	0.0000
4	zero	-	-	-	-	-	-
5	- 0.0010	- 0.0010	- 0.0010	- 0.0008	- 0.0002	0.0007	0.0009
6	zero	-	-	-	-	-	-
7	- 0.0031	- 0.0031	- 0.0031	- 0.0032	- 0.0035	- 0.0036	- 0.0038
8	zero	-	-	-	-	-	-
9	- 0.0026	- 0.0026	- 0.0026	- 0.0026	- 0.0026	- 0.0026	- 0.0027
10	zero	-	-	-	-	-	-

Appendix

Calculation of the Remanent Field

It is first necessary to establish the harmonic coefficients of the field in the aperture due to dipole current element  $\pm I$  separated (a) azimuthally to give a radially directed moment or magnetic direction and (b) radially to give an azimuthal moment.

(a) Azimuthal dipole

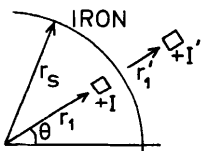


FIG. A1

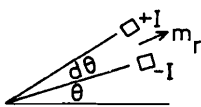


FIG. A2

Considering only the first quadrant of the magnet section, the rest being implied by the appropriate symmetry, and analysing the effect of a single current  $I$  at  $(r, \theta)$  into its Fourier component gives

$i_n = \frac{4}{\pi} \frac{I}{r_1} \cos n\theta$  / per unit length, in the notation and method of a previous report<sup>9</sup>, where  $n$  must be odd for a dipole magnet. Additionally, due to the image current in the iron, see Fig. A1,

$$i'_n = \frac{4}{\pi} \frac{I'}{r_1} \cos n\theta, \text{ with } I' = \left(\frac{\mu-1}{\mu+1}\right)I \text{ and } r_1 r'_1 = r_s^2$$

Hence for the vector potentials in the aperture

$$i_n a_n = \frac{\mu_0}{2n} \left( \frac{i_n}{r_1^{n-1}} + \frac{i'_n}{(r_1')^{n-1}} \right) = \frac{2\mu_0 I}{\pi n} \left( \frac{1}{r_1^n} + \left(\frac{\mu-1}{\mu+1}\right) \left(\frac{r_1}{r_s^2}\right)^n \right) \cos n\theta \dots 1,$$

Differentiate azimuthally,  $\frac{1}{r} \frac{\partial}{\partial \theta}$ , and multiply by  $r d\theta$ , which by superposition is equivalent in effect to dipole currents  $\pm I$  separated by  $r d\theta$ , Fig. A2, whence

$$\Delta i_n a_n = \frac{-2\mu_0 I}{\pi} \left( \frac{1}{r_1^{n+1}} + \left(\frac{\mu-1}{\mu+1}\right) \frac{r_1^{n-1}}{r_s^{2n}} \right) \sin n\theta r_1 d\theta$$

$$= \frac{-2\mu_0 m_r}{\pi} \left( \frac{1}{r_1^{n+1}} + \left(\frac{\mu-1}{\mu+1}\right) \frac{r_1^{n-1}}{r_s^{2n}} \right) \sin n\theta, \text{ where } m_r = I r_1 d\theta$$

If  $m_r = M_r r dr d\theta$ , where  $M_r$  is the magnetic moment/unit vol, then the total effect of the winding is obtained from

$$i_n a_n = \frac{-2\mu_0}{\pi} \iint_{\text{coil nodd}} M_r \left( \frac{1}{r^{n+1}} + \left(\frac{\mu-1}{\mu+1}\right) \frac{r^{n-1}}{r_s^{2n}} \right) \sin n\theta r dr d\theta \dots 2,$$

where the double integral is taken over the quarter winding

(b) Radial dipole

Proceeding as before, but differentiate equation 1 radially, Fig. A3, to obtain

$$\Delta_1 \alpha_n = \frac{2\mu_0 m_\theta}{\pi} \left( \frac{1}{r_1^{n+1}} - \frac{(\mu-1)}{(\mu+1)} \frac{r_1^{n-1}}{r_s^{2n}} \right) \cos n\theta, \quad \text{since } m_\theta = -I dr,$$

Hence the integrating over the coil

$${}_1 \alpha_n = \frac{2\mu_0}{\pi} \iint_{\text{coil}} M_\theta \left( \frac{1}{r^{n+1}} - \frac{(\mu-1)}{(\mu+1)} \frac{r^{n-1}}{r_s^{2n}} \right) \cos n\theta r dr d\theta \dots \dots 3,$$

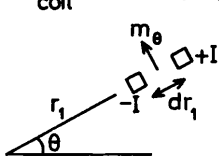


FIG. A3

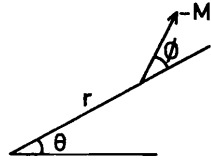


FIG. A4

If there is a moment  $-M/\text{unit vol}$  directed along a field direction  $\phi$ , Fig.4, which determines the orientation of the remanent dipoles, then the total  ${}_1 \alpha_n$  is given by resolving and adding the component effects as given by 2 & 3 to obtain

$${}_1 \alpha_n = \frac{-2\mu_0}{\pi} \iint_{\text{coil}} M \left[ \left( \frac{1}{r^{n+1}} - \frac{(\mu-1)}{(\mu+1)} \frac{r^{n-1}}{r_s^{2n}} \right) \cos n\theta \sin \phi - \left( \frac{1}{r^{n+1}} + \frac{(\mu-1)}{(\mu+1)} \frac{r^{n-1}}{r_s^{2n}} \right) \sin n\theta \cos \phi \right] r dr d\theta$$

$$= \frac{2\mu_0}{\pi} \iint_{\text{coil}} M \left( \frac{1}{r^{n+1}} - \frac{(\mu-1)}{(\mu+1)} \right) \sin(n\theta - \phi) r dr d\theta \dots \dots 4.$$

The angle  $\phi$  is a function of radius, and for a sector coil having substantially only the  $n = 1$  component of field in the windings,  $\tan \phi = P \cot \theta$  where

$$P = \frac{-4r + 3r_2 + 3E(r_2 - r_1) + r_1^3 r^{-2}}{-2r + 3r_2 + 3E(r_2 - r_1) - r_1^3 r^{-2}}$$

and  $E$  is the field enhancement factor due to the iron  $B = B_{\text{coil}}(1 + E)$ , where  $r_1$  &  $r_2$  are the inner and outer radii of the coil respectively.

In the present computations of equation 4,  $M$  is taken as constant and equal to  $j_c \lambda d/4$  for a square side of  $d$ , or  $0.81 j_c \lambda d/4$  for a round filament of diameter  $d$ . These expressions assume that the filaments are fully penetrated in a symmetrical mode and carry the critical current density  $j_c$ . The space factor  $\lambda$  is the sectional area of the filaments per unit area of the winding space. For remanent fields at low or zero excitation, the factor  $(\mu - 1)/(\mu + 1)$  in equation 3 will be equal to one, but for AC3 having no iron it is zero as is the enhancement factor  $E$ .

Approximate treatment

To obtain a fairly good estimate of the fields in the aperture it is reasonable for a thin coil without iron ( $\mu = 1$ ) to put  $M_\theta = 0$  since the average direction of the field in the winding is roughly radial. Making this assumption, equation 2 can then be integrated directly to obtain

$${}_1 \alpha_n = \frac{2\mu_0}{\pi} M_r \left[ \frac{\cos n\theta}{n} \right]_{\theta_1}^{\theta_2 \text{ etc.}} \frac{1}{n-1} \left( \frac{1}{r_1^{n-1}} - \frac{1}{r_2^{n-1}} \right)$$

with  ${}_1 \alpha_1 = \frac{2\mu_0}{\pi} M_r \left[ \cos \theta \right]_{\theta_1}^{\theta_2 \text{ etc.}} \ln r_2/r_1,$  for  $n \neq 1,$

and  $\theta_1, \theta_2$  etc. in the limits refer to the angular boundaries of the coil.

Using values for AC3 to illustrate these simplified formulae,  $r_1 = 0.050$  m,  $r_2 = 0.085$  m,  $\lambda = 0.15$ ,  $d = 8 \times 10^{-6}$  m and  $j_c = 1.0 \times 10^{10}$  Am<sup>-2</sup>, gives a

dipole field  $B_1 = {}_1 \alpha_1 = +0.515$  mT, a

sextupole field at full aperture

$$B_3 = -3 {}_1 \alpha_3 r_1^2 = +1.05$$
 mT,

decapole field at full aperture

$$B_5 = -5 {}_1 \alpha_5 r_1^4 = -0.30$$
 mT.

The harmonic ratios, which are independent of the value assigned to  $M$ , or  $J_c d$ , are then  $C_1/C_3 = 0.49$  and  $C_5/C_3 = -0.29$